Available online at www.sciencedirect.com
SCIENCE DIRECT®

Journal of the European Ceramic Society 24 (2004) 595–602

www.elsevier.com/locate/jeurceramsoc

Ferroelastic switching in a soft lead zirconate titanate

J.S. Forrester*, E.H. Kisi

School of Engineering, University of Newcastle, Callaghan NSW 2308, Australia

Received 5 December 2002; received in revised form 4 March 2003; accepted 6 April 2003

Abstract

Poled and unpoled ferroelectric lead zirconate titanate (“soft” PZT) samples were subjected to incremental compressive stresses up to 270 MPa to examine the mechanisms by which this type of ceramic responds to large static loads. Data indicate abundant ferroelastic switching leading to substantial non-linear deformation in the region 10–60 MPa. The ferroelastic switching is time dependent leading to creep under DC or static loading conditions. The creep is transient in nature and modelled reasonably well by an Andrade power law, initially increasing with increasing stress, however above 30 MPa, exhaustion of the creep mechanism reduces the creep rate. The creep exponent is 0.16 ± 0.03 at most stresses. Above 60 MPa, the ceramic responds as a linear elastic solid; however, there is evidence that the elastic constants change at applied stresses of greater than 90 MPa. No reverse switching occurred during unloading causing the final state of the ceramic to be mechanically poled transverse to the stress axis.

Keywords: Creep; Domain switching; $Pb(Zr,Ti)O_3$; Ferroelastic domain switching; Mechanical properties; PZT

1. Introduction

Ferroelectric materials are widely used in industrial, military, health care and domestic applications, including piezoelectric ignition devices, ultrasonic transducers, micro-positioning devices, high-dielectric-constant capacitors, explosive-to-electrical transducers, wide-aperture electro-optic shutters, colour filters, and ferroelectric RAM.[1–3] Polycrystalline $Pb_1Zr_{(1-x)}Ti_{(x)}O_3$ (PZT) ceramics, especially those compositions around the morphotropic phase boundary (Zr:Ti ratio of ~53:47), are popular due to their simplicity, compact size, low cost and high reliability.[4] The Curie temperature (T_c) is composition-dependent and can vary from ~190 to 490 °C.[5] PZT ceramics sinter at low temperature and form solid solutions with many other oxides allowing a wide range of properties to be developed. PZT can have high electromechanical coupling coefficients ($k_T \cong 50\%$, $k_{33} \cong 75\%$), large piezoelectric coefficients (d_{ij} ~200–700 pC/N), and a large range of dielectric constants ($K \sim 1000$–5000).[6,7] By judicious doping, the material may be rendered soft (easily poled) or hard (more difficult to pole). More widespread use of PZT has been impeded by their non-linear mechanical response and relatively low fracture toughness.

Ferroelectric materials are now being applied to load-bearing applications such as actuators.[8] This has increased the importance of understanding their mechanical properties over a wide range of loads and as a function of time. It is widely known that PZT and other ferroelectrics have a non-linear mechanical response that is also somewhat time-dependent. This has often been incorrectly referred to as non-linear elastic behaviour; however, it actually arises from the phenomenon of ferroelasticity or mechanically instigated domain reorientation. Ferroelasticity is of great interest in this field as it has been proposed that it makes a contribution to the fracture toughness of ferroelectric and other ceramics.[9–11] Fett and Munz have presented a comprehensive study of the elastic constants of three poled and unpoled commercial PZT ceramics including a critical appraisal of the many techniques used to measure them.[12] Care was taken to apply loads very quickly (20 MPa/s) in order to minimise the influence of any time dependence. Fett et al.[13] conducted tension and compression tests on commercial PZT samples. It was concluded that PZT shows non-symmetric stress–strain

* Corresponding author.
E-mail address: jforrest@mail.newcastle.edu.au (J.S. Forrester).

0955-2219/03/$ - see front matter © 2003 Elsevier Ltd. All rights reserved.
doi:10.1016/S0955-2219(03)00247-4

behaviour under tension and compression. In addition to ferroelastic domain switching, phase transformations were suggested as a likely mechanism for the non-linear behaviour observed. Schäufele and Härdtl investigated both hard and soft PZT samples with a range of compositions spanning the MPB during compression tests.[14] The samples had been previously electrically poled along the compression axis. Strains were measured with a linear resolution of 1 μm using 6 mm samples giving a strain resolution of $\sim 167\times10^{-6}$. Simultaneous depolarisation measurements were made. Considerable non-linear or plastic strain was observed during the testing and was attributed to ferroelastic domain switching in the materials. Soft PZT samples (Nd doped) showed no reversion of the domain switching on unloading whereas hard PZT samples (Fe doped) showed some reversal of domains during unloading. Such changes, tantamount to transverse mechanical poling of the ceramic, must have a profound influence on the piezoelectric properties of the material. Tai and Kim[15] have reported the degradation of piezoelectric properties as a result of sine wave loading at 20 Hz to maximum loads of approximately half of the fracture strength of the ceramic. X-ray diffraction evidence is used to support the explanation that the degradation is due to ferroelastic reorientation within the polycrystals. Although there is qualitative agreement between these papers, there is no quantitative link that explains why the ferroelasticity occurs in a single load cycle in one case[13,14] and requires many thousands of cycles in the other.[15]

We report here the response of polycrystalline unpoled and electrically poled PZT materials to the application of compressive loads. Loads were varied from zero to close to the fracture strength of the material and held at incremented steps in order to study time-dependant phenomena.

2. Experimental

The material tested is a "soft" ferroelectric PZT (doped with La and Sn) purchased from TRS Ceramics (TRS600). The manufacturer has supplied the following physical properties for poled polycrystals: a principal piezoelectric coupling coefficient $d_{33}=675$ pC/N, axial electromechanical coupling coefficient $k_{33}=0.76$, Curie temperature $T_c=190$ °C, elastic stiffness coefficients $Y_{11}^E=64$ GPa, $Y_{33}^E=47$ GPa, and Poisson's ratios $\sigma_{12}^E=0.26$, $\sigma_{13}^R=0.39$. Rietveld refinement of very high-resolution neutron diffraction patterns[16] has shown these materials to contain both the tetragonal phase ($a=4.0613(1)$ $c=4.0903(3)$) and rhombohedral phase ($a=4.0765(3)$ Å and $\alpha=89.92°$) in approximately equal proportions. The pseudo-cubic lattice parameters and two-phase nature of the samples makes them appear metrically cubic using standard laboratory X-ray diffraction equipment as no peak splitting or shoulders are visible in the diffraction patterns.

The samples were cylinders 10 mm in diameter and 15 mm high. These dimensions were selected as suitable to minimise misalignment in the loading, and to optimise the count rate in an accompanying neutron diffraction study. Similar mechanical loading experiments have shown that these studies can be performed using a variety of geometries.[17,18] This size also provides a suitable surface area on which to attach strain gauges. Two kinds of sample were used for the loading experiments (1) unpoled, i.e. of notionally[1] random crystallographic orientation and (2) electrically poled along the long-axis of the cylinder. Compressive loads were applied (under force control) to the samples using a compact 200 kN screw-driven, universal testing machine. The machine is designed to fit onto the medium resolution powder diffractometer at the high-flux Australian reactor (HIFAR) at Lucas Heights. The samples were short-circuited by the frame of the testing machine. Compression testing was chosen rather than the more usual 4-point bend tests applied to ceramics because Fett and Munz have determined that far more reliable estimates for the elastic and other material constants are obtained from tests where the sample is in a homogeneous stress state.[12] Strains were measured by strain gauges attached to the samples in the longitudinal (vertical) direction and in the transverse (horizontal) direction, and the macroscopic strain was recorded every 30 s for the duration of each experiment ($\sim$2 days). The resolution of the strain gauges and recording equipment used is 0.8×10^{-6} although analysis of the long-term stability, noise and load controller stability indicates that the actual precision is approximately $5–10\times10^{-6}$. Soft cadmium foil shims were placed between the sample and the hardened steel compression platens of the instrument in an attempt to accommodate any minor misalignment.

The samples were loaded stepwise at intervals, initially of 10 MPa, to a maximum of 270 MPa.[2] The stress was held constant at each interval for approximately 2 h while strain and neutron diffraction data were recorded. The samples were also unloaded stepwise and data was collected in the same way. The load–unload cycle was then repeated in order to compare differences between the first and subsequent loading events. Fewer stress steps were taken at higher stresses, during unloading and during reloading, as the rate of change of strain was less.

[1] Rietveld analyses indicate that the unpoled samples have an initial texture, presumably induced by the manufacturing process.

[2] The fracture strength had been previously determined to be approximately 330 MPa.

3. Results

3.1. Unpoled samples

Typical raw strain gauge data from longitudinal and transverse gauges attached to an unpoled sample are shown in Fig. 1. This is an unusual method of presenting data of this type, but the raw strain gauge data illustrates the strong time dependence at low load. The stress–strain curve derived from the strain at the end of each load step in Fig. 1 is plotted in Fig. 2a. As foreshadowed by previous work,[13,14] there are two distinct types of behaviour visible in Figs. 1 and 2a. Initially, there is an abrupt increase in strain at relatively low stress. Considerable non-linear deformation occurs in the region 10–60 MPa due to the ferroelastic re-orientation of domains within the samples. At higher stresses, the rate of strain accumulation decreases, and the strain steps become smaller and more uniform. For example, the longitudinal gauges indicate strains of 2×10^{-3} in the first 50 MPa and then only another 2×10^{-3} in the interval 50–270 MPa. This latter region, where the stress–strain curve in Fig. 2a becomes relatively straight, is indicative of purely elastic behaviour. After the maximum stress of 270 MPa was reached, the load was stepped back to zero. The unloading curve was relatively linear (elastic) and retraced the loading curve until, at approximately 60 MPa, the two diverge and the strain did not return to zero. There are few signs of non-linearity during unloading, whereby it can be concluded that, within the resolution of the measurement, only elastic strains were relaxed and little reverse domain switching occurred. Residual strains on unloading remained at approximately 900×10^{-6} (0.09%) for the transverse gauges and 1400×10^{-6} (0.14%) for the longitudinal gauges. These residual strains indicate the degree of ferroelastic switching or mechanical poling induced by the deformation. This point is addressed in a later section. It is important to note that during the initial accumulation of strain in Fig. 1, the process was highly time dependent. This creep-like behaviour will also be analysed in detail in a later section.

Raw strain vs. time data recorded during the second load-unload cycle are shown in Fig. 3 and the stress–strain curve derived therefrom is given in Fig. 4. Initial

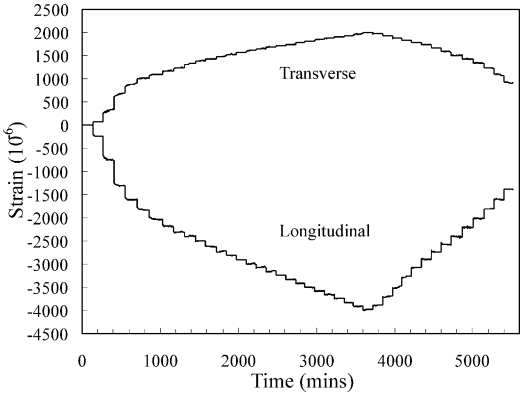

Fig. 1. Raw data from longitudinal and transverse strain gauges attached to the unpoled sample.

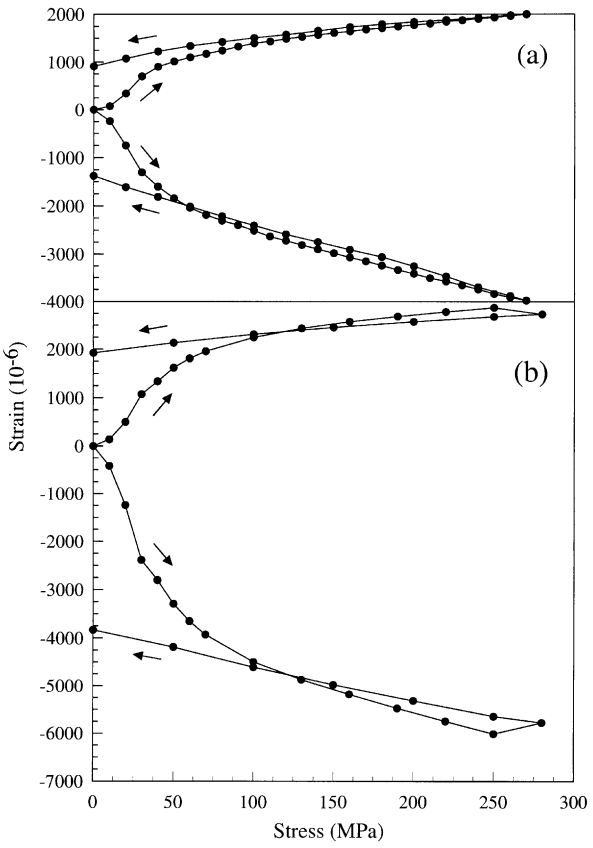

Fig. 2. Stress–strain curves derived from the end points of each constant stress hold in the strain-time data (e.g. Fig. 1) by averaging over gauge pairs. (a) Unpoled sample, note the abrupt increase at low stress and the linear regions at higher loads and during unloading. (b) Poled sample. The slight decrease in strain in the last load step may be due to micro-cracking as this sample was loaded slightly higher than the previous sample.

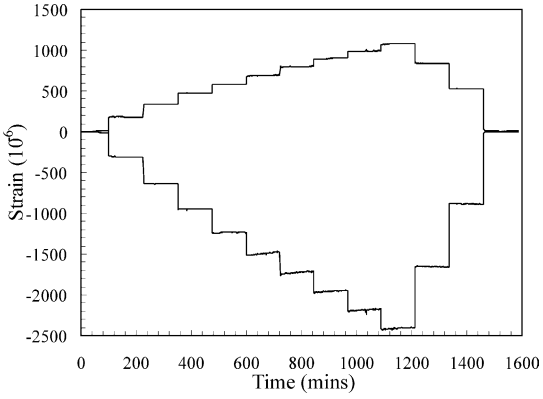

Fig. 3. Strain versus time data for an unpoled PZT loaded to 270 MPa following the initial loading cycle. There are few signs of non-linearity in contrast with the first cycle.

Table 1
Elastic constants[a]

Sample state	Modulus (GPa)		ν	Source
Unpoled (low load)	Y^E_{iso}	59	0.35 (2)	This work
Mechanically poled (<90 MPa)[b]	Y^E_{11}	97 (2)	0.54 (4)	This work
(>90 MPa)	Y^E_{11}	120 (2)	0.39 (4)	This work
Mechanically poled[c]	Y^E_{11}	108 (3)	0.34 (3)	This work
Unpoled (PIC151)	Y^E_{iso}	63–68	0.374	Fett and Munz (12)
Electrically poled parallel (PIC151)	Y^E_{33}	45.6		Fett and Munz (12)
Electrically poled perpendicular (PIC151)	Y^E_{11}	54–66		Fett and Munz (12)
Unpoled and poled		130–50		Fett et al. (26)
Electrically poled parallel (TRS600)	Y^E_{33}	47	$\sigma^E_{13}=0.39$	TRS ceramics (5)
Electrically poled perpendicular (TRS600)	Y^E_{11}	64	$\sigma^E_{12}=0.26$	TRS ceramics (5)

[a] Figures in parentheses are the estimated uncertainties in the last significant figure.
[b] Initially unpoled sample.
[c] Initially electrically poled sample.

strain values were set to zero before plotting. There are marked differences between the initial and repeat loading cycles (Figs. 3 and 4 compared with Figs. 1 and 2a). First, the large initial increase in strain is not evident in Figs. 3 and 4. Second, the slope of the stress–strain curve does not appear to change greatly during loading, and when the load is returned to zero, the strain likewise returns to zero. Taken together, these indicate that there is little or no ferroelastic switching after the first load cycle. Third, in Fig. 3, the strain remains relatively constant during each constant stress hold, indicating that there is no significant creep during reloading. There is a slight change in the slope of Fig. 4 at about 90 MPa that is addressed in the section relating to elastic properties below.

3.2. Poled samples

The same tests conducted on samples that had been previously electrically poled along the loading direction gave qualitatively similar results. The stress–strain curve for a poled sample is shown in Fig. 2b. Quantitative differences between the poled and unpoled samples are visible by comparison with Fig. 2a. The plastic strains in the poled samples are approximately twice as large as in the unpoled sample. Data collected during the second loading of the poled sample are not shown, as they are essentially identical to Figs. 3 and 4. That is, once mechanically poled, the electrically poled state is completely removed and the properties of the ceramic will not return to the original state.

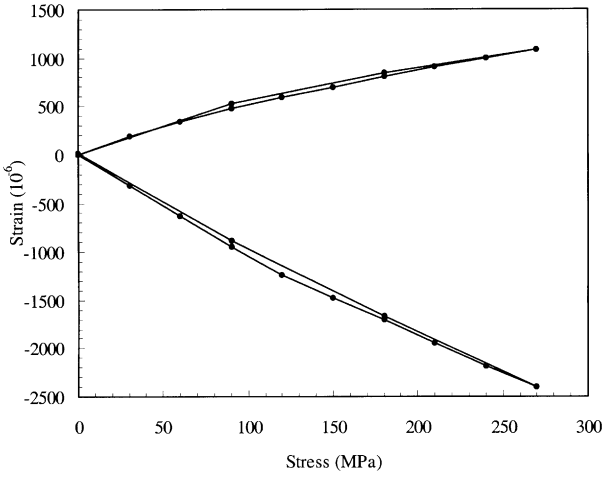

Fig. 4. Stress–strain curve of the initially unpoled sample derived from Fig. 3.

3.3. Elastic properties

The data in Figs. 2 and 4 allow us to examine the elastic response of the material for large static deflections. Several sample states are available for study. The low load region is characteristic of the as-sintered state in unpoled samples. In this region, we attempted to use the very first data points in Figs. 1 and 2 to isolate the elastic strains (not time dependent) from the ferroelastic (or plastic) strains that are time dependent. The elastic modulus obtained using this strategy is Y^E_{iso} [3] for unpoled samples and is given in Table 1 along with the corresponding Poisson's ratio.

The high load regions of Fig. 2 and the reload data in Fig. 4 are characteristic of the mechanically poled state and yield estimates for Y^E_{11}. Since the data in Fig. 2 contain a mixture of elastic and plastic deformation, the data in Fig. 4 have been used to extract the elastic modulus and Poisson's ratio[4]. Recognising that there is possibly a slight change in slope in Fig. 4, elastic constants both below and above 90 MPa have been calculated and are given in Table 1 along with some values from

[3] Strictly not an isotropic constant since even the unpoled samples have an initial non-random crystal orientation (see previous footnote).
[4] In this case a mixture of σ^E_{12} and σ^E_{13}.

the literature and also the manufacturer's specifications. It is particularly interesting to note the Poisson's ratio of approximately 0.5 below 90 MPa, in agreement with the incompressibility observed by Hwang and Waser.[19]

3.4. Time dependence (creep)

The time dependence of the strains is of great interest and worthy of closer inspection. To facilitate this, the time dependence of the first six load increments recorded by a longitudinal gauge and a transverse gauge are shown in Fig. 5. Each is zeroed to begin at the origin. The following observations can be readily made:

1. Some creep is apparent even at the lowest stress of 10 MPa.
2. The creep rate falls rapidly with time at constant stress, indicating that the creep mechanism is locally consumed during the process—as is typical of primary or transient creep.
3. At higher stresses the creep strains tend to saturate within the 2 h that the stress was held constant.
4. The creep rate and amount of strain accumulated in each load step is strongly stress dependent—initially increasing with increasing stress, but later decreasing. This indicates that, in addition to local saturation of the mechanism at constant load (see 3), there is global saturation of the mechanism associated with the accumulation of a limiting amount of plastic strain.

The creep data for two transverse and longitudinal gauges were fitted using the equation

$$\varepsilon = \varepsilon_o + \beta t^n \quad (1)$$

where β and n are fitted parameters. The strain at the start of a load step, ε_o is the instantaneous elastic part of the strain. Since the elastic constants change as a result of the mechanical poling, a linear approximation was used for Y^E ranging from the manufacturers Y^E_{33}(47 MPa) at 10 GPa to our measured value in Table 1 for mechanically poled samples (97 MPa) at 60 MPa. The equation fits the data relatively well in most cases, except in the longitudinal gauges at intermediate loads, perhaps due to the inadequacy of the linear approximation used to estimate ε_o.

Table 2 contains fitted values of the parameters β and n as a function of stress and Fig. 6 illustrates trends in these parameters for the unpoled sample. The constant β, which scales the magnitude of the creep strain, initially rises with increasing stress and then decreases as the creep mechanism is exhausted. The exponent n, that reflects the rate of saturation of the creep mechanism, mostly lies close to 0.16(3) in unpoled samples and 0.11(3) in poled samples, apart from a few outlying points. There may be an upward trend in n at higher stresses.

4. Discussion

The results presented here agree with and extend those previously given by Schäufele and Härdtl con-

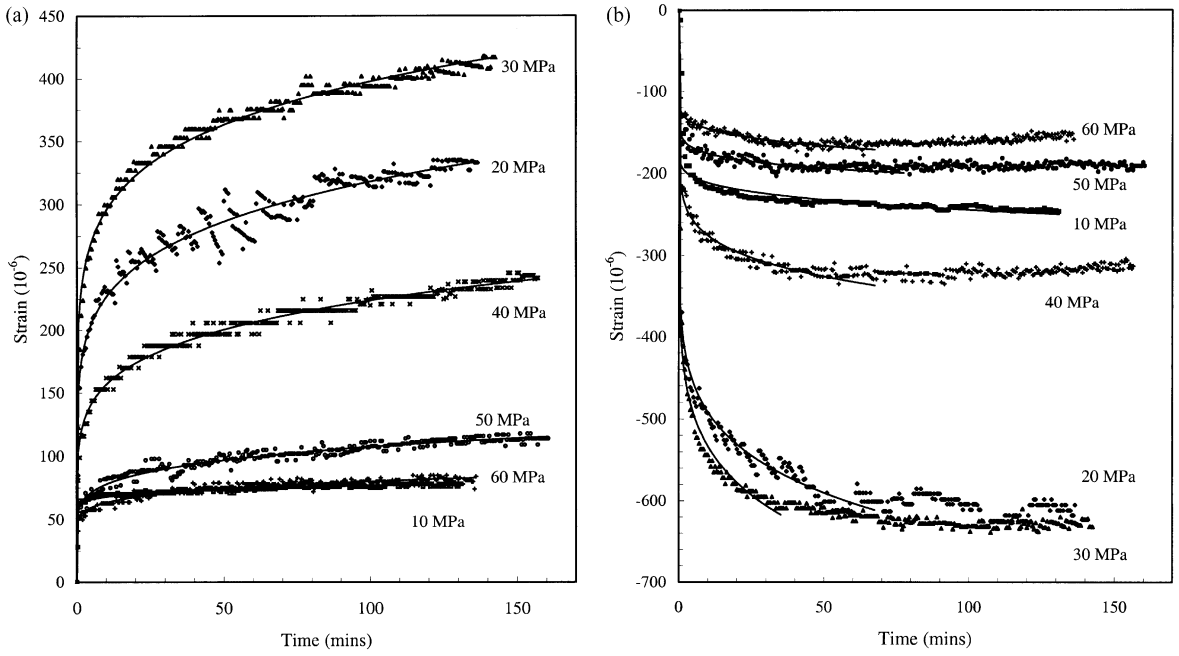

Fig. 5. The initial six load steps in (a) a transverse gauge and (b) a longitudinal gauge in the unpoled sample illustrating time dependent behaviour. Data are shown as points and the solid lines are fits to the initial transient using Eq. (1).

cerning the mechanical behaviour of PZT in compression.[14] Soft PZT ceramics very readily undergo ferroelastic domain reorientation under an applied stress. In the materials used here, it is apparent from a comparison of the loading and unloading curves in Fig. 2 that some irreversible deformation occurs even during the first 10 MPa stress increment. This is reinforced in Fig. 5 where a small amount of creep is apparent. We are therefore unable to accurately determine the critical stress for ferroelasticity, σ_c, in our samples. It can be noted however that the small amount of creep at 10 MPa indicates that it lies not far below this value. Likewise, the time dependence observed here, coupled with the high strain rates used by Schäufele and Härdtl make it difficult to determine the critical stress for their samples however, from their published data it would also appear to be of order 10 MPa. The ferroelastic strains measured in this work (3.5×10^{-3} poled and 1.4×10^{-3} unpoled) are considerably lower than those of Schäufele and Härdtl ($\sim6\times10^{-3}$), however they are in good agreement with the following estimates of the maximum strains allowed by a domain reorientation mechanism. High-resolution neutron diffraction has shown that the samples are a mixture of the rhombohedral and tetragonal phases in approximately equal proportion.[16] The lattice parameters indicate maximum ferroelastic strains of 7.38×10^{-3} for a perfectly oriented tetragonal domain and 2.05×10^{-3} for a perfectly oriented rhombohedral domain leading to a maximum ferroelastic strain, for a hypothetical perfectly oriented sample, of $\sim4.7\times10^{-3}$.

Table 2
Creep parameters β and n for unpoled and PZT poled

Stress (MPa)	Longitudinal Gauge 1 β	Longitudinal Gauge 2 β	Transverse Gauge 1 β	Transverse Gauge 2 β
Unpoled				
10	13	21	10	9
20	153	236	120	67
30	214	280	181	127
40	97	102	76	66
50	54	45	26	33
60	32	24	21	21
	N	*n*	*N*	*N*
10	0.282	0.267	0.193	0.136
20	0.128	0.158	0.178	0.154
30	0.136	0.152	0.147	0.143
40	0.157	0.176	0.194	0.153
50	0.247	0.152	0.224	0.19
60	0.291	0.243	0.181	0.235
Poled				
10	312	12	97	21
20	760	124	287	162
30	654	337	300	239
40	344	316	185	178
50	152	201	103	107
60	81	131	59	61
	N	*n*	*n*	*n*
10	0.143	0.144	0.086	0.137
20	0.108	0.112	0.072	0.082
30	0.11	0.086	0.088	0.103
40	0.125	0.107	0.122	0.155
50	0.185	0.186	0.161	0.197
60	0.188	0.229	0.175	0.232

4.1. Domain switching and mechanical poling

The macroscopic strains indicate that the poled sample has more than twice the population of switchable domains of the unpoled sample. Regardless of whether a poled or unpoled sample is used, there is still a wide distribution of crystal orientations present in the material, derived from the distribution of crystal orientations in the cubic parent phase during production of the ceramic. In the tetragonal phase, the switching angle is 90°, i.e. interchange of the *a* and *c* crystallographic axes. In the rhombohedral phase, the ferroelastic switching that occurs is presumed to be of the kind that transforms the slightly longer $[111]_R$ into any of the slightly shorter $\{11\text{-}1\}_R$. The angle between closest pairs of $\{111\}_R$ poles in this pseudo-cubic structure is approximately 70.5°. In the absence of local stress inhomogeneities, switching is favourable (i.e. leads to a net decrease in the sample length) for any $[001]_T$ oriented within approximately 45° or any $[111]_R$ oriented within approximately 35° of the stress axis. We assume there is a minimum threshold (or critical) stress, σ_c, directed along $[001]_T$ or $[111]_R$ of the domain, below which no ferroelasticity can occur. It would therefore be expected that the minimum applied stress for switching a particular

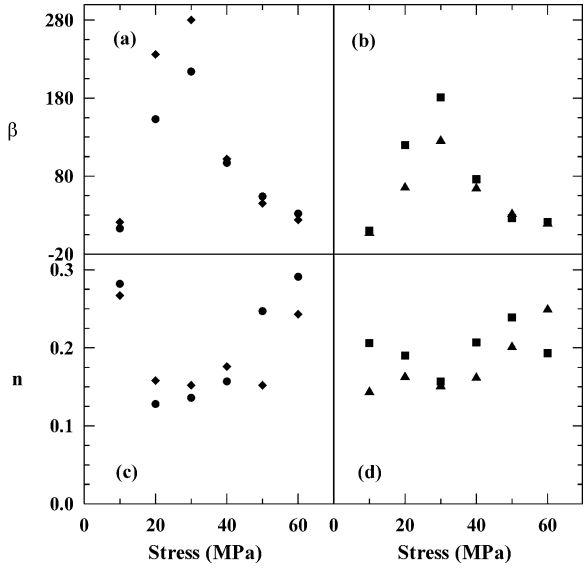

Fig. 6. Creep parameters β and n from data recorded in individual (a, c) longitudinal and (b, d) transverse strain gauges of the unpoled PZT loaded in the range 10–60 MPa.

domain, making an angle ϕ with the applied stress, would be given by:

$$\sigma_{appl} = \sigma_c/\cos^2\phi \quad (2)$$

Given that a small amount of ferroelasticity is already observed at 10 MPa, we can assume σ_c to be just less than 10 MPa, say 9 MPa. Applying Eq. (2) we expect that, if σ_c is homogeneous throughout the sample, all rhombohedral domains can be switched at applied stresses of greater than ~13 MPa and all tetragonal domains at ~18 MPa. The fact that considerable ferroelasticity occurs in our samples well above these stresses indicates that the distribution of σ_c values in the samples is much wider than that due to domain orientation effects alone i.e. there are considerable variations in the degree of domain wall pinning.

4.2. Creep

Unlike the high temperature creep of ceramics, room temperature creep is a rare occurrence. The phenomenon has been studied in magnesia partially stabilised zirconia (Mg–PSZ) loaded in tension above 240 MPa[20] and in ceria stabilised tetragonal zirconia polycrystals (Ce–TZP) loaded in compression above 1200 MPa.[10] In both those instances, creep was caused by a tetragonal to monoclinic phase transformation. Creep has also been observed in yttria stabilised tetragonal zirconia polycrystals (Y-TZP) subjected to compressive stresses exceeding 1700 MPa due to ferroelastic reorientation of tetragonal domains.[18] Fett and Thun[21,22] have determined the creep behaviour of a commercial soft PZT in tensile tests, and evaluated the parameters n and β [Eq. (1)]. The time dependent deformation observed in the current samples in compression is another example of room temperature ceramic creep at very low stresses. Whilst the theoretical framework for understanding time dependent ferroelasticity exists in the time dependent Landau–Ginzburg theory (see for example Salje[23]), the two-phase polycrystalline samples used in this work are too far removed from a single crystal for quantitative analyses to be made.

The kinetics of stress relaxation in unpoled PZT was studied by Esaklul et al.[24] using three-point bend loads followed by incremental unloading. It is difficult to make a connection between this work and Esaklul et al. as (1) their samples were "hard" PZT, (2) the samples were open circuit during the experiment, and (3) their test equipment was operated under length control.

The creep is of differing importance in applications. AC applications are largely unaffected due to the slow time constant of the ferroelasticity. In addition, the creep behaviour observed here verifies that the elastic constant data of Fett and Munz,[12] collected at 20–30 MPa/s were largely unaffected by time dependent strains. DC applications on the other hand are dominated by the creep behaviour until it saturates. In the saturated or mechanically poled state, the electrical and mechanical properties of the ceramic are quite different to those of the as-received ceramic, particularly for initially electrically poled materials. This places limitations on the maximum repeatable piezoelectric strain and may necessitate a re-evaluation of poling strategies for load-bearing applications.

4.3. Mechanical properties and longevity

Ferroelasticity has been proposed as a toughening mechanism in some zirconia ceramics (e.g. Y3–TZP[11] and has gained some support from in-situ neutron diffraction studies[18,25] although this hypothesis has not gained general acceptance due to the very high critical stress. For the PZT in this study the converse is true, i.e. the critical stress is so low that the ferroelastic effect has saturated well before the material fails. Therefore, at the more critical higher stresses when micro-cracks are expected to develop, the mechanism is inoperative.

The degradation of electrical and mechanical properties due to mechanical cycling (fatigue) has been attributed to ferroelastic domain re-orientation.[15] In that work, the fatigue life of unpoled samples was greater than for poled samples due to the greater amount of re-orientation required to convert the (longitudinal) electrically poled state into the (transverse) mechanically poled state and the attendant internal stresses generated. It would appear that, in a purely mechanical sense, the longevity of the ceramics would be maximised by initially either mechanically or electrically poling them transverse to the applied stress axis, although at a considerable cost in the available piezoelectric strain.

Acknowledgements

Thanks are due to the Australian Research Council small grants scheme for scholarship funding (J.F.), the Australian Institute of Nuclear Science and Engineering and Dr. Andrew Studer of the Neutron Scattering group at the Australian Nuclear Science and Technology Organisation.

References

1. Lysne, P. C. and Percival, C. M., Analysis of shock-wave-actuated ferroelectric power supplies. *Ferroelectrics*, 1976, **10**, 129–133.
2. Newnham, R. E. and Ruschau, G. R., Smart electroceramics. *J. Am. Ceram. Soc.*, 1991, **74**, 463–480.
3. Toyoshima, H. and Kobatake, H., Features and applications of FeRAM. *NEC Research and Development*, 1999, **40**, 206–209.
4. Haertling, G. H., Ferroelectric ceramics: history and technology. *J. Am. Ceram. Soc.*, 1999, **82**, 797–818.
5. TRS Ceramics: Product Specifications 1998. Pennsylvania, USA.

6. Jaffe, B., Cook, W. R. and Jaffe, H., *Piezoelectric Ceramics*. Academic Press, New York, 1971.
7. Park, S.-E. and Shrout, T. R., Characteristics of relaxor-based piezoelectric single crystals for ultrasonic transducers. *IEEE Trans. on Ultrasonics, Ferroelectrics and Frequency Control*, 1997, **44**, 1140–1147.
8. Zhang, Z. and Raj, R., Influence of grain size on ferroelastic toughening and piezoelectric behaviour of lead zirconate titanate. *J. Am. Ceram. Soc*., 1995, **78**, 3363–3366.
9. Virkar, A. V. and Matsumoto, R. L. K., Ferroelastic domain switching as a toughening mechanism in tetragonal zirconia. *J. Am. Ceram. Soc*., 1986, **69**, 224–226.
10. Kisi, E. H., Kennedy, S. J. and Howard, C. J., Neutron diffraction observations of ferroelastic domain switching and tetragonal-to-monoclinic transformation in Ce–TZP. *J. Am. Ceram. Soc*., 1997, **80**, 621–628.
11. Garg, A. and Goel, T. C., Mechanical and electrical properties of PZT ceramics (Zr:Ti = 0.40:0.60) related to Nd^{3+} addition. *Materials Science & Engineering B-Solid State Materials for Advanced Technology*, 1999, **60**, 128–132.
12. Fett, T. and Munz, D., Measurement of Young's Moduli for lead zirconate titanate (PZT) ceramics. *J. Testing and Evaluation*, 2000, **28**, 27–35.
13. Fett, T., Müller, S., Munz, D. and Thun, G., Nonsymmetry in the deformation behaviour of PZT. *J. Mater. Sci. Lett*., 1998, **17**, 261–265.
14. Schäufele, A. B. and Härdtl, K. H., Ferroelastic properties of lead zirconate titanate ceramics. *J. Am. Ceram. Soc*., 1996, **79**, 2637–2640.
15. Tai, W.-P. and Kim, S.-H., Relationship between cyclic loading and degradation of piezoelectric properties in $Pb(Zr,Ti)O_3$ ceramics. *Mater. Sci. and Eng*., 1996, **B38**, 182–185.
16. Kisi, E. H., Kennedy, S. J. and Forrester, J. S., *J. Phys: Condensed Matter* (in preparation).
17. Chan, C.-J., Lange, F. F., Rühle, M., Jue, J.-F. and Virkar, A. V., Ferroelastic domain switching in tetragonal zirconia single crystals—microstructural aspects. *J. Am. Ceram. Soc*., 1991, **74**, 807–813.
18. Ma, Y., Kisi, E. H. and Kennedy, S. J., Neutron diffraction study of ferroelasticity in a 3 mol%Y_2O_3–ZrO_2. *J. Am. Ceram. Soc*., 2001, **84**, 399–405.
19. Hwang, S. C. and Waser, R., Study of electrical and mechanical contribution to switching in ferroelectric/ferroelastic polycrystals. *Acta Mater*., 2000, **48**, 3271–3282.
20. Finlayson, T. R., Gross, A. K., Griffiths, J. R. and Kisi, E. H., Creep of Mg–PSZ at room temperature. *J. Am. Ceram. Soc*., 1994, **77**, 617–624.
21. Fett, T. and Thun, G., Determination of room-temperature tensile creep of PZT. *J. Mater. Sci. Letters*, 1998, **17**, 1929–1931.
22. Munz, D. and Fett, T., *Ceramics, Failure, Material Selection, Design*. Springer-Verlag, März, 1999.
23. Salje, E., *Phase transitions in ferroelastic and co-elastic crystals*. Cambridge University Press, Cambridge, 1990.
24. Esaklul, K. A., Gerberich, W. W. and Koepke, B. G., Stress relaxation in PZT. *J. Am. Ceram. Soc*., 1980, **63**, 25–30.
25. Cain, M. G., Bennington, S. M., Lewis, M. H. and Hull, S., Study of the ferroelastic transformation in zirconia by neutron diffraction. *Philos. Mag. B*, 1994, **69**, 499–507.
26. Fett, T., Munz, D. and Thun, G., Young's modulus of soft PZT from partial unloading tests. *Ferroelectrics*, 2002, **274**, 67–81.